

Electronic structure of solid coronene: differences and commonalities to picene

Taichi Kosugi^{1,2}, Takashi Miyake^{1,2}, Shoji Ishibashi¹, Ryotaro Arita^{2,3,4}, and Hideo Aoki⁵

¹Nanosystem Research Institute “RICS”, AIST, Umezono, Tsukuba 305-8568, Japan

²Japan Science and Technology Agency, CREST, Honcho, Kawaguchi, Saitama 332-0012, Japan

³Department of Applied Physics, University of Tokyo, Hongo, Tokyo 113-8656, Japan

⁴PRESTO, Japan Science and Technology Agency (JST), Kawaguchi, Saitama 332-0012, Japan and

⁵Department of Physics, University of Tokyo, Hongo, Tokyo 113-0033, Japan

We have obtained the first-principles electronic structure of solid coronene, which has been recently discovered to exhibit superconductivity with potassium doping. Since coronene, along with picene, the first aromatic superconductor, now provide a class of superconductors as solids of aromatic compounds, here we compare the two cases in examining the electronic structures. In the undoped coronene crystal, where the molecules are arranged in a herringbone structure with two molecules in a unit cell, the conduction band above an insulating gap is found to comprise four bands, which basically originate from the lowest two unoccupied molecular orbitals (doubly-degenerate, reflecting the high symmetry of the molecular shape) in an isolated molecule but the bands are entangled as in solid picene. The Fermi surface for a candidate of the structure of K_x coronene with $x = 3$, for which superconductivity is found, comprises multiple sheets, as in doped picene but exhibiting a larger anisotropy with different topology.

PACS numbers: 74.20.Pq, 74.70.Kn, 74.70.Wz

Introduction — Discovery of superconductivity in solid picene doped with potassium atoms [1] is seminal and came as a surprise in that the picene, on top of the highest T_c among organic superconductors, belongs to *aromatic* compounds, the most typical, textbook class of organic materials. Then a natural question to ask is: can other aromatic compounds become superconducting as well? Before examining this question, let us first briefly summarize the known superconductors in wider, carbon-based materials. First discovery goes back to 1965, when a graphite-intercalation compound (GIC), KC_8 , was found to be a superconductor at 0.1 K [2], and the highest T_c among GIC's to date is 11.6 K in CaC_6 [3]. Fullerene is another class, where potassium-doped fullerene, K_3C_{60} , is a superconductor with $T_c = 20$ K [4], followed by Cs_2RbC_{60} with $T_c = 33$ K [5], or 40 K in Cs_3C_{60} under 15 kbar [6]. In the last decade, the boron-doped diamond [7] joined carbon-based superconductors. The first aromatic superconductivity in the potassium-doped solid picene discovered by Kubozono's group[1] was unsuspected, since the (undoped) solid of picene (a hydrocarbon compound with five benzene rings connected in a zigzag) has been known to be a good insulator, as naturally expected for a solid of aromatic molecules. For the doped K_x picene two superconducting phase, with $T_c = 7$ K and 18 K respectively, are reported at around $x \simeq 3$.

The present authors reported for the first time the first-principles electronic structure of both undoped and doped solid picene in the framework of the density functional theory (DFT) within the local density approximation (LDA) [8]. We have revealed the following: For the undoped solid picene, where picene molecules are arranged in a herringbone structure with two molecules in a unit cell, (i) the conduction band consists of four

bands, which originate basically from the lowest two unoccupied molecular orbitals (LUMO and LUMO+1) in an isolated picene molecule, but the bands are entangled. (ii) When doped with potassium atoms, two things happen to electronic as well as crystal structures: the herringbone structure is deformed, and the electronic wave function significantly spills from the organic molecules' LUMO's into potassium sites[8].

Now, if we come back to the question of whether and which other aromatic compounds can become superconducting, recently Kubozono's group found superconductivity in doped coronene [9]. Coronene, $C_{24}H_{12}$, is another of typical aromatic molecules, with seven benzene rings assembled in a concentric disk. Superconductivity in K_x coronene is reported to appear around $x \simeq 3$ with T_c up to 15 K.[10] Motivated by this, here we have obtained the electronic structure of solid coronene, both undoped and doped. An obvious interest is the differences and commonalities between the crystal and electronic structures of solid coronene as compared with those of solid picene. This is precisely the purpose of the present work. The obtained results are analyzed with maximally-localized Wannier functions (WF's) [16], in terms of which we downfold the system into a tight-binding model and compare with those for picene.

We shall show that the conduction band of the undoped solid coronene comprises four bands, which basically originate from the lowest two unoccupied molecular orbitals (doubly-degenerate, reflecting the symmetry of the molecule higher than that of picene) in an isolated molecule, but the bands are entangled as in solid picene. The Fermi surface for a candidate of the structure of K_x coronene with $x = 3$, for which superconductivity is found, comprises multiple sheets, as in doped picene but exhibiting a more one-dimensional character with differ-

ent topology.

The present electronic structure will serve as a basis for discussing mechanisms of the superconductivity. Since some classes of organic superconductors are considered to have an electronic mechanism,[11] picene and coronene superconductors may possibly belong to them. There have been some theoretical studies[14, 15] that suggest that solid picene is a strongly correlated electron system. As for the electron-phonon coupling, on the other hand, Kato *et al.* estimated the phonon frequencies and the electron-phonon coupling for various hydrocarbon molecules[12]. For picene they found that the electron-phonon coupling can be as large as 0.2 eV. While it is generally difficult to quantitatively estimate T_c for a phonon mechanism due to the ambiguity of the Coulomb pseudopotential (μ^*), they concluded that $T_c \sim 10$ K may be expected. For coronene, the coupling is estimated to be about 0.1 eV. Subedi *et al.*[13] recently calculated the phonon spectrum and electron-phonon interaction for solid picene, and they found that the electron-phonon coupling is sufficiently strong to reproduce the experimental T_c of 18 K within the Migdal-Eliashberg theory.

First-principles bands — The calculation is based on DFT, where LDA in the Perdew-Zunger formula is adopted for the exchange-correlation energy functional [17]. We use the projector-augmented wave (PAW) method [18], implemented to the Quantum Materials Simulator (QMAS) package [19]. The pseudo Bloch wave functions are expanded by plane waves up to an energy cutoff of 40 Ry with $4 \times 6 \times 4$ k -points.

As for the crystal structure, here we adopt the lattice parameters of natural coronene (karpatite) reported by Echigo *et al.* [21]. Natural coronene has a monoclinic (space group: $P2_1/a$) structure with $a = 16.094$, $b = 4.690$ and $c = 10.049$ Å, and $\beta = 110.79^\circ$. We have also performed calculations adopting the lattice parameters of synthetic coronene [22], and have confirmed that the results are essentially unchanged from those for the natural coronene. The molecular solid has a herringbone arrangement of molecules as depicted in Fig. 1 with a unit cell containing two molecules (centered respectively at $(0, 0, 0)$ and $(1/2, 1/2, 0)$ as dictated by the symmetry). The lattice parameters are fixed at the experimental values, and the internal atomic positions are optimized. The angle between the planes of the inequivalent molecules in the optimized geometry is 95° , which agrees with the measured value. We have also found that the point-group symmetry D_{6h} for an isolated coronene molecule is lowered to D_{2h} in the crystal.

Figure 2 displays the electronic band structure of coronene. We have an insulator with a band gap of 2.41 eV. The gap, which is naturally smaller than the HOMO-LUMO gap, calculated to be 2.90 eV, of an isolated coronene molecule, is indirect, with the valence band top located at Y in the Brillouin zone, while the conduction band bottom at Γ . Since the crystal structure is layered, where the herringbone arrangement, on the $a - b$ plane, of the molecules are stacked along the c axis, the

electronic structure is more dispersive along $a^* - b^*$ axis. More precisely, the dispersion along b^* is larger than that for a^* , which directly reflects the distance between neighboring molecules being shortest along b . The conduction band, with a width of 0.40 eV, consists of four bands derived from the doubly-degenerate, e_{1g} LUMO's. For solid picene by comparison, the conduction band, with a width 0.39 eV, consists of four bands with a band gap of 2.36 eV, while the LUMO-HOMO gap of a picene molecule is 2.96 eV. These are similar to solid coronene, where a difference is the conduction band of the solid picene originates from LUMO and LUMO+1 of an isolated picene molecule [8]. The valence band of solid coronene has a width of 0.45 eV, and consists of four bands, which is shown to be derived from the (again doubly-degenerate) e_{2u} HOMO's of an isolated coronene molecule.

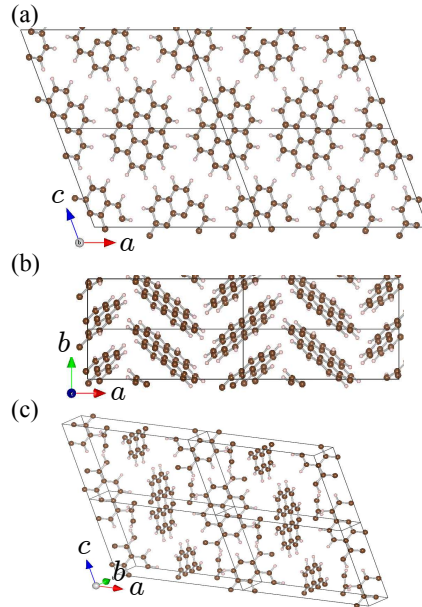


FIG. 1: (Color online) Crystal structure of undoped solid coronene viewed along (a) b axis, (b) c axis and (c) a bird's eye view. Solid lines delineate unit cells.

Downfolding — In order to construct an *ab initio* tight-binding model, we have constructed the maximally-localized Wannier functions [16] from the four-fold conduction band. The DFT-LDA bands have turned out to be accurately reproduced, as seen in Fig. 3(a). On this finer energy scale we can see that the four bands are bunched into two, nearly degenerate ones. The density of states (DOS) has a dip (at around half-filling $x = 2$ in the rigid band picture), and has a peak around 0.2-0.3 eV below that. These features contrast with the DOS for the solid picene [8]. Figure 3(b,c) depict the major transfer integrals in the downfolded tight-binding model.

If we turn to wave functions, shown in Fig. 4, two out of four WF's, which we denote by w_h and w_l , are centered at one coronene molecule in the unit cell, while the other two at the other molecule. The difference in the orbital

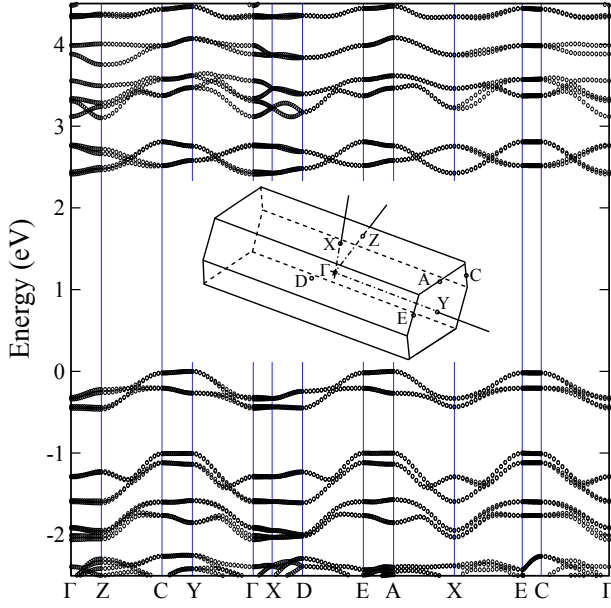


FIG. 2: (Color online) Calculated electronic band structure of the undoped crystalline coronene. The origin of the energy is set to be the valence band top. The inset depicts the Brillouin zone with Γ , Z, C, Y, X, D, E and A respectively corresponding to $(0, 0, 0)$, $(0, 0, 1/2)$, $(0, 1/2, 1/2)$, $(0, 1/2, 0)$, $(1/2, 0, 0)$, $(1/2, 0, 1/2)$, $(1/2, 1/2, 1/2)$ and $(1/2, 1/2, 0)$ in units of $(\mathbf{a}^*, \mathbf{b}^*, \mathbf{c}^*)$.

energy, $\varepsilon_h - \varepsilon_l$, between the two WF's is 18.2 meV, which is to be compared with 11.3 meV for solid picene. In Fig. 4 we also display the two-fold degenerate LUMO's for an isolated molecule with b_{3g} and b_{2g} , respectively, in the D_{2h} symmetry. We can now notice that w_h is derived mainly from b_{3g} orbital while w_l from b_{2g} .

Doped solid coronene — Let us finally discuss the doped coronene. If we naively adopt a rigid-band picture for a doping level of $x = 3$ for which superconductivity is observed, the Fermi surface (not shown) consists of multiple surfaces that comprise one-dimensional (planar) surfaces and a two-dimensional (cylindrical) one, along with a more three-dimensional one. However, since we have shown for the doped picene[8] that the rigid-band picture is broken in this material for two-fold reasons (i.e., a distorted herringbone structure upon doping along with a spilling of the molecular wave function over to potassium sites), we should have a look at the electronic structure of the coronene actually doped with K. Since the structure of the doped system has not been experimentally obtained, we have tried a structural optimization of K_3 coronene. Since this in itself is an important but vast task, here we only show a candidate structure. We started from a plausible geometry with one potassium atom just above the molecule and two in the interstitial region. The initial coordinates of the six potassium atoms we adopted are $(1/2, 0, 0)$, $(0, 1/2, 0)$, $(\pm 1/3, 1/2, \pm 1/3)$ and

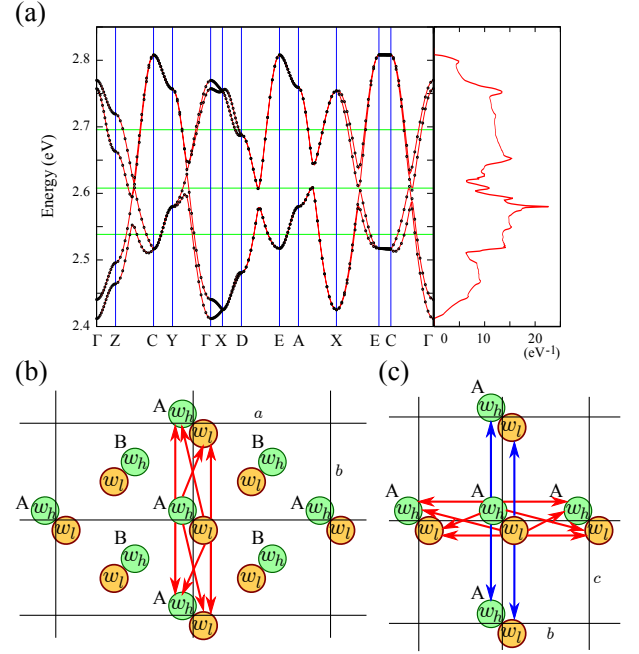


FIG. 3: (Color online) (a) Band structure and the density of states for the conduction bands of the undoped, solid coronene. Dots are the LDA result, while curves those from the maximally-localized Wannier function procedure. Horizontal lines respectively indicate Fermi levels for $x = 1, 2, 3$ in the rigid band picture. Lower panels depict the transfer integrals t estimated from the Wannier orbitals on the $a-b$ plane (b) and $b-c$ plane (c), where the red (blue) arrows represent the transfer integrals with $|t| > 30$ meV ($10 < |t| < 30$ meV).

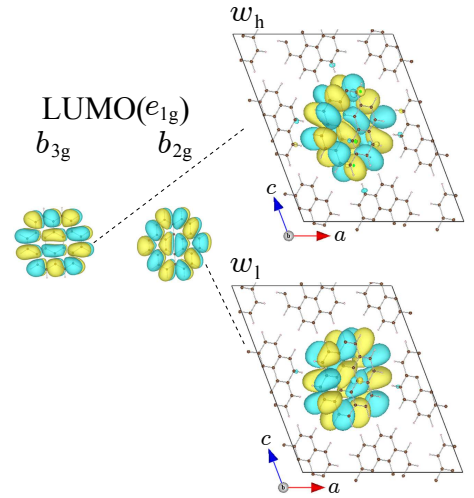


FIG. 4: (Color online) The two-fold degenerate LUMO's (left panel) in an isolated coronene molecule are compared with the maximally-localized Wannier functions w_l (w_h) with a lower-energy (higher-energy) constructed for the conduction bands of the undoped solid coronene.

$(\pm 5/6, 0, \pm 1/3)$, which preserve the monoclinic symmetry. Interestingly, the optimization, with the lattice parameters fixed at those for the pristine structure, resulted in a significant rearrangement of the herringbone structure with the monoclinic symmetry lowered, along with a strong deformation of each molecule, as displayed in Fig. 5. We can see that the resultant Fermi surface is a composite of one-dimensional surfaces (i.e., multiple pairs of planar surfaces). The doped picene also has a coexistence of multiple Fermi surfaces[8], but the doped coronene has topology of the surface different from those in doped picene, which comes from different (and more one-dimensional) tight-binding structure (Fig. 3(b,c)). A more elaborate structural optimization is needed for an accurate description, and the details will be reported elsewhere.

Finally, a few words about the “aromaticity” of molecules. Its simplest definition is in terms of the “Clar sextets” (resonating benzene rings)[23] on a given molecular structure. When a molecule is fully benzenoid (where the sextets exhaust all the double bonds) the wave function tends to be localized on the sextets. In this picture picene is non-fully-benzenoid, while coronene, also non-fully-benzenoid, has multiple Clar structures.[22] The relation of these quantum chemical properties with band structures is another of interesting future problems.

In summary, we have studied the electronic structure of solid coronene by means of first-principles calculation. The conduction band is found to comprise four bands, which basically originate from the lowest two unoccupied molecular orbitals (doubly-degenerate, reflecting the molecular symmetry) in an isolated molecule, but the bands are entangled as in solid picene. Then the maximally-localized Wannier functions are used to derive a downfolded tight-binding Hamiltonian, where the major transfer integrals are found to significantly differ from those in solid picene. The Fermi surface for a candidate of the structure of K_x coronene with $x = 3$, for which superconductivity is found, comprises multiple sheets, as in doped picene but with different topology of the surface. Their relevance to superconductivity is an interesting future problem.

We are indebted to Yoshihiro Kubozono for letting us know of the experimental results prior to publication. The present work is partially supported by the Next Generation Supercomputer Project, Nanoscience Program from MEXT, Japan, and by Grants-in-aid No. 19051016 and 22104010 from MEXT, Japan and the JST PRESTO program. The calculations were performed at the supercomputer centers of ISSP, University of Tokyo, and at the Information Technology Center, University of Tokyo.

-
- [1] R. Mitsuhashi, Y. Suzuki, Y. Yamanari, H. Mitamura, T. Kambe, N. Ikeda, H. Okamoto, A. Fujiwara, M. Yamaji, N. Kawasaki, Y. Maniwa, and Y. Kubozono, *Nature* **464**, 76 (2010).
 - [2] N. B. Hannay, T. H. Geballe, B. T. Matthias, K. Andres, P. Schmidt, and D. MacNair, *Phys. Rev. Lett.* **14**, 225 (1965).
 - [3] T. E. Weller, M. Ellerby, S. S. Saxena, R. P. Smith and N. T. Skipper, *Nature Phys.* **1**, 39 (2005); N. Emery, C. Hérod, M. d’Astuto, V. Garcia, Ch. Bellin, J. F. Maréché, P. Lagrange and G. Loupías, *Phys. Rev. Lett.* **95**, 087003 (2005).
 - [4] A. F. Hebard, M. J. Rosseinsky, R. C. Haddon, D. W. Murphy, S. H. Glarum, T. T. M. Palstra, A. P. Ramirez and A. R. Kortan, *Nature* **350**, 600 (1991).
 - [5] K. Tanigaki, T. W. Ebbesen, S. Saito, J. Mizuki, J. S. Tsai, Y. Kubo and S. Kuroshima, *Nature* **352**, 222 (1991).
 - [6] T. T. M. Palstra, O. Zhou, Y. Iwasa, P. E. Sulewski, R. M. Fleming and B. R. Zegarski, *Solid State Commun.* **93**, 327 (1995).
 - [7] E. A. Ekimov, V. A. Sidorov, E. D. Bauer, N. N. Melfnik, N. J. Curro, J. D. Thompson, and S. M. Stishov, *Nature* **428**, 542 (2004).
 - [8] T. Kosugi, T. Miyake, S. Ishibashi, R. Arita and H. Aoki, *J. Phys. Soc. Jpn.* **79**, 044705 (2010).
 - [9] Y. Kubozono, M. Mitamura, X. Lee, X. He, Y. Yamanari, Y. Takahashi, Y. Suzuki, Y. Kaji, R. Eguchi, K. Akaike, T. Kambe, H. Okamoto, A. Fujiwara, T. Kato, T. Kosugi, and H. Aoki, submitted.
 - [10] X. F. Wang, R. H. Liu, Z. Gui, Y. L. Xie, Y. J. Yan, J. J. Ying, X. G. Luo and X. H. Chen, arXiv:1102.4075v1 (unpublished), have reported that K_x phenanthrene also exhibits superconductivity with $T_c \simeq 5$ K.
 - [11] See, e.g., K. Kuroki, *J. Phys. Soc. Jpn.* **75**, 051013 (2006).
 - [12] T. Kato and T. Yamabe, *J. Chem. Phys.* **115**, 8592 (2001); T. Kato, K. Yoshizawa and K. Hirao, *J. Chem. Phys.* **116**, 3420 (2002); T. Kato and T. Yamabe, *Chem. Phys.* **325**, 437 (2006).
 - [13] A. Subedi and L. Boeri, arXiv:1103.4020v1 (unpublished).
 - [14] G. Giovannetti and M. Capone, *Phys. Rev. B* **83**, 134508 (2011).
 - [15] M. Kim, B. I. Min, G. Lee, H. J. Kwon, Y. M. Rhee and J. H. Shim, arXiv:1011.2712v1 (unpublished).
 - [16] N. Marzari and D. Vanderbilt, *Phys. Rev. B* **56**, 12847 (1997); I. Souza, N. Marzari and D. Vanderbilt, *Phys. Rev. B* **65**, 035109 (2001).
 - [17] D. M. Ceperley and B. J. Alder, *Phys. Rev. Lett.* **45**, 566 (1980); J. P. Perdew and A. Zunger, *Phys. Rev. B* **23**, 5048 (1981).
 - [18] P. E. Blöchl, *Phys. Rev. B* **50**, 17953 (1994); G. Kresse and D. Joubert, *Phys. Rev. B* **59**, 1758 (1999).
 - [19] <http://www.qmas.jp/>
 - [20] K. Hummer and C. Ambrosch-Draxl, *Phys. Rev. B* **72**, 205205 (2005).
 - [21] T. Echigo, M. Kimata and T. Maruoka, *American Mineralogist* **92**, 1262 (2007).
 - [22] T. M. Krygowski, M. Cyrański, A. Ciesielski, B. Świrski and P. Leszczyński, *J. Chem. Inf. Comput. Sci.* **36**, 1135 (1996).
 - [23] E. Clar, *Polycyclic Hydrocarbons*, Academic Press, London.

don, 1964

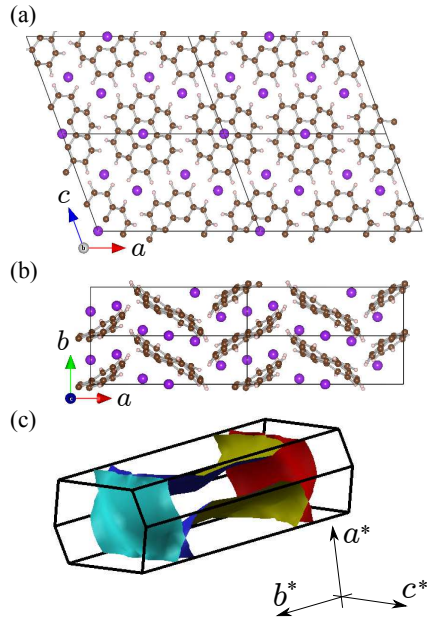


FIG. 5: (Color online) Crystal structure of K_3 coronene viewed along (a) b or (b) c axis. Larger balls represent K atoms. The Fermi surface for the K_3 coronene is displayed in (c).